HHS Public Access

Author manuscript

Cytoskeleton (Hoboken). Author manuscript; available in PMC 2016 January 13.

Published in final edited form as:

Cytoskeleton (Hoboken). 2014 June ; 71(6): 380–394. doi:10.1002/cm.21181.

Arf1 and Arf6 Promote Ventral Actin Structures formed by acute Activation of Protein Kinase C and Src

Juliane P. Caviston[*], **Lee Ann Cohen**[*], and **Julie G. Donaldson**

Cell Biology and Physiology Center, NHLBI, NIH, Bethesda, MD

Abstract

Arf proteins regulate membrane traffic and organelle structure. Although Arf6 is known to initiate actin-based changes in cell surface architecture, Arf1 may also function at the plasma membrane. Here we show that acute activation of protein kinase C (PKC) induced by the phorbol ester PMA led to the formation of motile actin structures on the ventral surface of Beas-2b cells, a lung bronchial epithelial cell line. Ventral actin structures also formed in PMA-treated HeLa cells that had elevated levels of Arf activation. For both cell types, formation of the ventral actin structures was enhanced by expression of active forms of either Arf1 or Arf6, and by the expression of guanine nucleotide exchange factors that activate these Arfs. By contrast, formation of these structures was blocked by inhibitors of PKC and Src, and required phosphatidylinositol 4, 5-bisphosphate, Rac, Arf6 and Arf1. Furthermore, expression of ASAP1, an Arf1 GTPase activating protein (GAP) was more effective at inhibiting the ventral actin structures than was ACAP1, an Arf6 GAP. This study adds to the expanding role for Arf1 in the periphery and identifies a requirement for Arf1, a “Golgi Arf”, in the reorganization of the cortical actin cytoskeleton on ventral surfaces, against the substratum.

Introduction

Cell behavior is influenced by environmental stimuli including cellular interaction with other cells and with the extracellular matrix. Epithelial cells organize into polarized layers, with cells joined together at the apical surface by adherens junctions and their basolateral surfaces exposed to the underlying matrix. During development, wound healing and tumor metastasis, cells in an epithelium undergo an epithelial to mesenchymal transition enabling cells to break away from their neighbors and rearrange their cell surface and underlying actin cytoskeleton to facilitate cell migration. Understanding how cells accomplish and regulate this dramatic change in cytoarchitecture is the focus of much research in cell and developmental biology. Although members of the Rho family of GTP-binding proteins are important for this process [Heasman and Ridley 2008], increasing evidence supports roles for Arf GTP-binding proteins in regulating the membrane traffic and membrane structure needed to support these events [D'SouzaSchorey and Chavrier 2006; Donaldson and Jackson 2011].

Corresponding author: Julie G. Donaldson, Cell Biology and Physiology Center, Bldg 50, Rm 2503, Bethesda, MD 20892, Tel 301-402-2907, Fax 301-402-1519, donaldsonj@helix.nih.gov.

*These authors contributed equally.

Arf6 regulates membrane traffic and influences the cortical actin cytoskeleton in the cell periphery. In HeLa cells, Arf6 is present at the plasma membrane (PM) and on endosomal membranes that are derived from clathrin-independent endocytosis (CIE). The CIE endosomal membrane system is distinct from yet intersects with endosomal membranes derived from clathrin-mediated endocytosis [Grant and Donaldson 2009]. A cycle of inactivation and activation of Arf6 is necessary for maturation of intracellular compartments containing internalized membranes and for their recycling back to the plasma membrane, respectively [Donaldson et al. 2009]. The recycled membrane contains integrins [Powelka et al. 2004] and other cell adhesion molecules [Eyster et al. 2009; Zimmermann et al. 2005], and is important for cell adhesion, cell spreading and wound healing [D'Souza-Schorey and Chavrier 2006]. Arf6-GTP can activate phosphatidylinositol 4-phosphate 5-kinase (PIP5-kinase) to generate phosphatidylinositol 4,5-bisphosphate (PIP_2) [Aikawa and Martin 2003; Brown et al. 2001; Honda et al. 1999], phospholipase D (PLD) to generate phosphatidic acid (PA) [Brown et al. 1993; Cockcroft et al. 1994], and interact with Rac guanine nucleotide exchange factors (GEFs) [Koo et al. 2007; Santy et al. 2005] to activate Rac, allowing Arf6 to influence the cell architecture at the PM. The generation of PIP_2 and activation of Rac can facilitate the formation of PM ruffles and protrusions. Additionally, cells expressing active Arf6 can polymerize actin on endosomal membranes leading to vesicle motility [Schafer et al. 2000]. These combined activities of Arf6 are important for the wide range of functions ascribed to Arf6 including cell adhesion [Palacios et al. 2001], cell spreading [Balasubramanian et al. 2007; Song et al. 1998], neurite outgrowth [Hernandez-Deviez et al. 2002; Hernandez-Deviez et al. 2004], podosome formation [Svensson et al. 2008], invasion [Hashimoto et al. 2004; Tague et al. 2004], migration [Santy and Casanova 2001], and metastasis [Sabe et al. 2009]. Although Arf6 is ubiquitously expressed, it is not abundant, raising the possibility that other Arf proteins might augment Arf6 activities.

Arfs 1–5 reversibly associate with the Golgi complex and dissociate into the cytosol in response to GTP-binding and GTP hydrolysis, respectively. At the Golgi, these Arfs regulate membrane trafficking within the ER-Golgi system and maintain the structure of the Golgi complex. In most cells, Arf1 is the most abundant Arf and is thought responsible for the recruitment of the coat proteins COPI to the early Golgi and clathrin adaptor proteins AP1, AP3, AP4 and the GGAs to the *trans* Golgi network [Donaldson et al. 2005]. Additionally, Arf1 can recruit and activate PI 4-kinase at the Golgi [Godi et al. 1999] and it has been shown to activate phospholipase D on Golgi membranes [Ktistakis et al. 1995]. Since Golgi-associated Arfs are released into the cytosol when in the GDP-bound form, they could potentially become activated at other cellular locations. In fact, it has been shown that Arf1 can activate PLD at the plasma membrane in human myeloid cells [Whatmore et al. 1996]. Recently, several studies have caused a shift in the paradigm of Arfs 1–5 working exclusively at the Golgi and Arf6 acting as the sole Arf functioning at the PM. Arf1 has been implicated in endocytosis of activated G protein-coupled recetors [Boulay et al. 2008; Daher et al. 2010] and of GPI-anchored proteins in some cells [Kumari and Mayor 2008]. Active Arf6 has been shown to lead to activation of Arf1 in the periphery [Cohen et al. 2007]. Sequential involvement of Arf6 and then Arf1 is observed during Fc-mediated phagocytosis [Beemiller et al. 2006]. We propose that some of the peripheral actin reorganization activities attributed to Arf6 might involve Arf1.

Arf6 has been implicated in the formation of podosomes and invadopodia [Svensson et al. 2008; Tague et al. 2004], specialized actin-based structures formed at the ventral surface of cells [Albiges-Rizo et al. 2009; Caldieri and Buccione 2010]. These structures form in various cell types and act as adhesion sites and sites for degradation of the extracellular matrix [Block et al. 2008]. The non-receptor tyrosine kinase Src plays a key role in regulating the formation of podosomes and invadapodia [Gavazzi et al. 1989]. Beas-2b cells, a lung epithelial cell line, form ventral, podosome-like structures after treatment with phorbol 12-myristate 13-acetate (PMA) [Xiao et al. 2009], a tumor promoter and known activator of protein kinase C and Src. Here we examine the role of Arf proteins in formation of these PMA-induced ventral actin structures in the Beas-2b and HeLa cells. We find that Arf1, known primarily as a “Golgi Arf” and, to a lesser extent, Arf6 are required for the formation of the ventral actin structures in both cell types, demonstrating that Arf1 can mediate actin reorganization at the plasma membrane.

Results

Beas-2b cells form PMA-stimulated ventral actin structures in an Arf-dependent manner

Beas-2b cells, immortalized human bronchial epithelial cells, are reported to form ventral, podosome-like structures after treatment with phorbol esters [Xiao et al. 2009]. In order to examine whether Arf proteins were involved in cortical actin structures, we incubated Beas-2b cells with PMA and observed that the cells, which normally exhibit extensive actin stress fibers, formed large ventral actin structures upon PMA treatment (Fig. 1A). We hypothesized that since Arf6 has a role in actin reorganization at the plasma membrane, expression of constitutively active forms of Arf6 may augment the basal level of activity present in this cell type. We found that expressing Arf6Q67L caused more PMA-treated cells to exhibit ventral actin structures (80% of cells compared to 42% of control cells) and the structures formed were more numerous (Fig. 1B) than those formed in untransfected cells (Fig. 1A) (see also Fig. S1 in Supplementary Materials). Remarkably, expression of activated Arf1, Arf1Q71L, also increased the percentage of cells making ventral actin structures, to 75% (Fig. 1C) and the structures were more numerous than in control cells (Fig. S1 in Supplementary Materials) but expression of a constitutively active form of Arf5 did not (unpublished observations). We also found that we could localize endogenous Arf1 and Arf6 to the ventral actin structures formed in PMA-treated Beas-2b cells (Fig. S2 in Supplementary Materials). It was notable in particular that endogenous Arf1 could be localized to the ventral actin structures (arrowhead) over its cytosolic distribution. Arf6, on the other hand, is present all along the cell surface and is only weakly enhanced on the ventral structures. Thus, in Beas-2b cells, the ability to form ventral actin structures in response to PMA is sensitive to the level of active Arf1 and Arf6 present in the cell.

To examine these PMA-induced ventral actin structures more closely using live cell imaging, we expressed LifeAct-RFP to label the actin and the GFP-tagged membrane marker (Mem-GFP), which we have previously used to mark the plasma membrane and endosomes associated with Arf6 and clathrin-independent endocytosis [Brown et al. 2001; Porat-Shliom et al. 2008]. Upon PMA addition, arcs of actin appeared on the ventral surface while stress fibers were diminished. The membrane marker, Mem-GFP, was not

concentrated with these actin structures; instead, it was evenly distributed along the ventral cell surface (Fig.1D and Movie1 in Supplementary Materials). Although actin accumulated along the ventral surface, there was no membrane fold or ruffle. These actin structures thus resembled ventral actin waves, first described in Dictyostelium where their formation and propagation has been linked to formation of phagocytic cups [Bretschneider et al. 2004]. More recently these actin waves have been observed in mast cells as either “standing” or “traveling” waves [Wu et al. 2013] and in some cells to be coupled to cycles of integrin engagement and detachment [Case and Waterman 2011].

We also examined Beas-2b cells expressing Arf6Q67L or Arf1Q71L in live cell imaging experiments. Cells expressing Arf6Q67L and Lifeact-RFP to visualize actin were imaged before and after PMA treatment. Expression of Arf6 Q67L was confirmed by co-expressing Mem-GFP, which marked the vacuole structures typical of Arf6 Q67L expression. LifeAct-RFP was seen in small actin polymerization foci at the ends of stress fibers prior to PMA treatment. After PMA was added (Fig. 1E, arrow) these small activities grew, and pushed radially out from their center. These structures were circular, and they grew outward away from their center (Fig.1E and Movie 2 in Supplementary Materials). Similar to Arf6Q67L, cells expressing Arf1Q71L-RFP and actin-GFP have increased nascent actin polymerization activities mostly near the ends of stress fibers and when treated with PMA these structures stabilized and grew, and numerous new structures formed (Fig. 1F and Movie 3 in Supplementary Materials). Notably, Arf1Q71L-RFP itself was recruited to the PM, and the membrane surrounding the actin structure when the Beas-2b cells were treated with PMA (Fig. 1F and Movie 3 in Supplementary Materials). The ventral actin structures that formed with either Arf6Q67L or Arf1Q71L were more numerous (see Fig. S1 in Supplementary Materials) and less dynamic than those formed in Beas-2b cells alone (Fig. 1D and Movie 1 in Supplementary Materials), likely reflecting the fact that these constitutively active Arfs were not normally cycling through GTP- and GDP-bound forms.

PKC and Src are required for PMA induced ventral ruffles

Phorbol esters activate PKC, which has been shown to lead to activation of Src in a number of cases [Brandt et al. 2003; Tatin et al. 2006.] To test whether PKC activity was required for ventral ruffle formation, we treated Beas-2b cells with PMA and the PKC inhibitor, GF109203x. The presence of the inhibitor during PMA treatment completely blocked ventral ruffle formation (Fig. 2A and B). These findings are consistent with others that showed PKC involvement in podosome formation upon phorbol ester treatment in human vascular endothelial [Tatin et al. 2006] and in Beas-2b [Xiao et al. 2010] cells.

Next, we checked whether the activity of Src or other Src family kinases were required for this response. Src family members phosphorylate and modulate the function of many proteins involved in regulating focal adhesions and particularly the linkage between focal adhesion structures and the actin cytoskeleton [Albiges-Rizo et al. 2009]. To determine if Src is involved in regulating the formation of PMA-induced ventral structures, we treated cells with PMA and the Src inhibitor PP2 and observed inhibition of ventral ruffle formation, while treatment with the related, but inactive, compound PP3 had no effect on ventral ruffle formation (Fig. 2A and B).

Ventral actin structures are blocked by inhibitors of Rac, Arf1 and Arf6 but not by BFA

Activated Arf6 leads to activation of Rac1 [Koo et al. 2007; Santy et al. 2005] and PIP5-kinase [Aikawa and Martin 2003; Brown et al. 2001; Honda et al. 1999]. Since many PM cortical actin rearrangements depend upon the activities of Rac [Boshans et al. 2000; Koo et al. 2007; Santy and Casanova 2001] and also the activities of PIP5-kinase to generate PIP_2 [Aikawa and Martin 2003; Brown et al. 2001], we examined whether inhibition of Rac or loss of PIP_2 would block the PMA stimulation of ventral actin structures. Expression of dominant negative Rac (RacT31N) or a 5-phosphatase, which depletes cells of PIP_2, blocked the formation of ventral actin structures (Fig. 2C and D). In addition, expression of either Arf6T27N or Arf1T31N blocked ventral actin structures (Fig. 2C and D). Since the expression of Arf1T31N leads to the disassembly of the Golgi complex and an impairment in function of the secretory pathway over 24 h [Dascher and Balch 1994], we also treated cells for short periods with brefeldin A (BFA), which blocks activation of Arf proteins by BFA-sensitive GEFs at the Golgi [Donaldson and Jackson 2011]. Remarkably, cells treated with BFA, which disrupted Golgi structure as evidenced by GM130 distribution, still formed ventral actin structures upon PMA stimulation (Fig. 2E), demonstrating that this role for Arf1 in the periphery is likely due to a BFA-insensitive peripheral GEF.

We next decided to examine whether expression of BFA-insensitive GEFs would increase the percentage of cells exhibiting ventral actin structures similar to what we observed upon expression of active forms of Arf1 and Arf6. EFA6 is an Arf GEF that localizes to the cell surface and primarily activates Arf6 [Brown et al. 2001; Cohen et al. 2007; Franco et al. 1999; Macia et al. 2001]. Expression of EFA6 led to a greater than 2-fold increase in the proportion of cells making the ventral actin structures (Fig. 3A and B). ARNO is another BFA-resistant Arf GEF, which can activate either Arf6 or Arf1 to varying degrees depending upon the assay and cellular context [Cohen et al. 2007; Santy et al. 2001]. ARNO family members (which also include Cytohesin and Grp1) are cytosolic GEFs that are recruited to membranes through their pleckstrin homology (PH) domains [Casanova 2007]. The PH domains bind to PIP_2 or phosphatidylinositol 3,4,5-trisphosphate (PIP_3) depending upon splice variants determined by the presence of 3 glycine or 2 glycine residues in the PIP binding pocket, respectively [Klarlund et al. 2000]. Remarkably, we found that expression of ARNO-3G (the splice form containing a PH domain which preferentially binds to PIP_2) was diffusely associated with the membrane but did not appreciably enhance formation of the ventral actin structures (Fig. 3A and B). In contrast, expression of ARNO-2G, the form recruited by PIP_3, was specifically present on the ventral structures and dramatically enhanced formation of the actin structures to over 90% of the cells in the population (Fig. 3A and B). This suggests that it is PIP_3, and the ability of ARNO-2G to be recruited to the membrane that enhances the response.

HeLa cells form ventral actin structures if cells have increased levels of Arf activation

Next, we wanted to determine whether other cells would also make ventral actin structures in response to PMA treatment so we tested this in HeLa cells, which we have used for many of our studies on Arf6 function. As in Fig. 1D, we expressed the GFP-tagged membrane marker (Mem-GFP) to mark the PM. Treatment of HeLa cells with PMA did not result in the formation of ventral actin structures as we had observed with Beas-2b cells (Fig. 4A and

B, top row and C), although there was a loss of actin stress fibers after PMA treatment. However, in cells expressing EFA6, PMA treatment caused a dramatic shift in the actin cytoskeleton from peripheral protrusions along the cell margins (Fig. 4A, second row) to actin structures along the ventral (bottom) surface, next to the substratum (Fig. 4B, second row). These actin structures appeared as ventral ruffles with EFA6 present on the membrane and F-actin behind the fold of membrane (Fig. 4B, second row, inset). This was a robust response with 67% of cells expressing EFA6 showing clear evidence of ventral ruffle formation as scored by phalloidin staining of fixed cells (Fig. 4C). In the absence of PMA, EFA6-expressing cells rarely formed ventral ruffles (Fig. 4A and C). The effect of EFA6 on ventral actin structures required a functioning GEF domain since expression of a catalytically inactive form of EFA6 (EFA6-EK), did not form ventral ruffles in response to PMA (Fig.4A and B, third row). We could also promote ventral actin structures in HeLa cells expressing ARNO, and as we saw in the Beas-2b cells, it was ARNO-2G (the PIP_3 binding form) that supported ventral structures to the same extent as EFA6 did, whereas ARNO-3G (the PIP_2 binding form) only weakly supported their formation (Fig. 4C).

Since HeLa cells did not make the ventral actin structures constitutively upon PMA treatment, they were an advantageous model system to test what factors could induce the actin ruffles. Given that expression of the BFA-insensitive Arf6 GEFs promoted these actin structures, we wondered whether active forms of Arf6 or Arf1 could also be involved. As was observed in Beas-2b cells, expression of activated forms of Arf6 or Arf1 could support robust ventral actin structures (Fig. 4B and C). The localization of these structures to the ventral surface of the cells could be clearly seen in Z-sections from stacked images of PMA-treated cells expressing EFA6 (Fig. 4D). While the actin and membrane marker were primarily distributed along the dorsal surface and protrusive edges of untreated cells, the cortical actin shifted down to the ventral surface of PMA-treated cells. Taken together, PMA-induced ventral ruffles formed in HeLa cells that had elevated Arf-GTP levels.

As was observed in Beas-2b cells, the ventral actin structures that formed in HeLa cells in response to PMA were dependent upon both PKC and Src activation. Treatment of HeLa cells with inhibitors of PKC (GF 109203x) or Src (PP2) blocked the formation of ventral structures in EFA6-expressing HeLa cells (see Fig. S3 in Supplementary Materials). In addition, the ventral structures were not formed in cells co-expressing EFA6 and RacT31N, Arf6T27N, Arf1T31N or the 5-phosphatase to eliminate PIP_2 (see Fig. S4 in Supplementary Materials) suggesting that the activities of Rac, Arf6, Arf1 and PIP_2 were required for formation of these actin structures. Another downstream effector of activated Arf6, phospholipase D [Brown et al. 1993; Cockcroft et al. 1994], was inhibited by addition of butanol [Jovanovic et al. 2006], and yet PMA-induced ventral ruffle formation was not blocked (unpublished observations), suggesting that PLD activity was not required.

In HeLa cells, ventral actin structures formed in cells transfected with constitutively active forms of Arf1 or Arf6. Both Arf1 and Arf6 can promote activation of Rac [Boshans et al. 2000; Koo et al. 2007; Lewis-Saravalli et al. 2013; Santy and Casanova 2001] and PIP5-kinase [Aikawa and Martin 2003; Brown et al. 2001; Honda et al. 1999]. Since formation of ventral actin structures was inhibited by expression of dominant negative form of Rac1 (T31N) or expression of a PIP 5-phosphatase that would deplete cells of PIP_2, we next asked

whether expression of constitutively active Rac1 or PIP5-kinase were sufficient to form these structures in HeLa cells in response to PMA. When HeLa cells were transfected with Rac1Q71L and treated with PMA, the cells did not form ventral actin structures, although untreated cells formed circular dorsal ruffles as expected (Fig. 5A). Cells transfected with PIP5-kinase did accumulate small endosomes but did not form ventral ruffles upon PMA treatment (Fig. 5B). Thus the activities of Rac1 and PIP5-kinase were necessary, but not sufficient, for HeLa cells to make ventral ruffles in response to PMA.

To obtain an appreciation of how these structures form over time in HeLa cells, cells expressing unlabeled EFA6, LifeAct-RFP to label F-actin, and Mem-GFP to mark the PM were imaged live before and after PMA treatment (Fig. 5C and Movie 4 in Supplementary Materials). In the absence of PMA treatment, actin was visible in active areas of protrusion at the lateral edge of the cell. Occasionally ventral actin structures formed in the untreated cells expressing EFA6, but these structures were short-lived and quickly dissipated (data not shown). After PMA addition (at time 0), it is clear that the membrane, labeled with Mem-GFP, was being pushed by the band of actin assembling behind it (Fig. 5 and Movie 4 in Supplementary Materials). This membrane ruffle distinguishes the ventral actin structures in the HeLa cells from those in the Beas-2b cells, which had no membrane associated with the actin wave. Most of the ventral ruffles that form in the PMA-treated cells formed within the first 10 min after treatment, and were persistent for the length of the movie (30 min). In EFA6-expressing cells, these ventral ruffles often had a crescent appearance, and were seen growing out radially away from the center of the crescent.

Although the requirements for PMA-induced actin structures were the same in HeLa and Beas-2b cells, the resultant ventral actin structures formed showed differences in membrane association. To further distinguish the ventral actin structures formed in HeLa and Beas-2b cells, we examined the distribution of cortactin and proteins associated with focal adhesions in cells making ventral actin structures. Cortactin was associated with both the ventral ruffles formed in EFA6-expressing HeLa cells (see Fig. S5A in Supplementary Materials) and the ventral actin waves in Beas-2b cells (see Fig. S5B in Supplementary Materials). Interestingly, in HeLa cells phospho-paxillin was not associated with the ruffle, but rather was moved to either side of the ruffle while in Beas-2b cells, phospho-paxillin was associated with the actin wave (see Fig. S5 in supplementary materials). Similarly, phosphorylated FAK was also moved to either side of the ventral ruffle in HeLa cells but was present in the actin wave in Beas-2b cells (see Fig. S5 in Supplementary Materials). These images also emphasize that both the ruffles and waves form on the ventral surface and that focal adhesion proteins present in the same focal plane are shifted out of the region of the ruffle in HeLa cells and incorporated into the wave in Beas-2b cells.

Knockdown of Arf1 inhibits ventral actin structures in Beas-2b and HeLa cells

We had observed that Arf1T31N could block ventral ruffle formation and active forms of Arf1 could enhance ruffle formation, however, overexpression of these mutant constructs could nonspecifically alter how other Arfs function in the cell. To garner support for a direct role of Arf1 in ventral wave formation, we depleted Beas-2b cells of Arf1 using siRNA. In Arf1-depleted cells PMA-induced ventral waves were reduced by 60% when compared to

control cells (Fig. 6B and C). Although Arf1 depletion impaired ventral wave formation, β-COP, a Golgi coat protein recruited by Arf-GTP, remained associated with the Golgi complex (Fig. 6A) in agreement with others [Volpicelli-Daley et al. 2005], suggesting that the Golgi and secretory pathway remained intact in cells depleted of Arf1 (Fig. 6A). This suggests that Arf1 plays a critical role in the actin re-arrangements that lead to ventral wave formation. In contrast, depletion of Arf6 caused a modest 30% decrease in the number of cells forming ventral waves when compared to control cells (Fig. 6C). We repeated the knockdown experiments in HeLa cells and observed similar results. Cells depleted of Arf1 showed a 60% inhibition in the ability to form ventral ruffles compared to control cells while cells depleted of Arf6 exhibited only a modest decrease (33%) in cells making ventral actin structures (see Fig. S6 in Supplementary Materials). Interestingly, cells depleted of Arf6 and expressing EFA6 still exhibited a loss of stress fibers, typically observed in EFA6-expressing cells [Franco et al. 1999], suggesting that EFA6 may affect other Arfs besides Arf6. Indeed although Arf6 is a preferential substrate for EFA6, a number of studies have shown that EFA6 can also activate Arf1 [Cohen et al. 2007; Franco et al. 1999; Macia et al. 2001].

As another approach to demonstrate the role of Arf1and Arf6 in ventral wave formation we expressed GAP proteins specific for either Arf1 or Arf6. ASAP1 is a GAP that is localized to focal adhesions and works preferentially on Arf1 [Brown et al. 1998; Liu et al. 2002]. ACAP1 is a GAP with specificity towards Arf6 [Jackson et al. 2000]. Expression of ASAP1 in Beas-2b cells significantly reduced the number of cells exhibiting ventral waves from 40% to less than 10% (Fig. 7A and B), while expression of the GAP-dead, arginine mutant of ASAP1 (ASAP1-RK) had only a modest effect (Fig. 7B). Expression of ACAP1 also inhibited the number of cells exhibiting ventral waves (from 40% down to 20%) whereas the GAP-dead mutant showed no significant effect (Fig. 7B). Indeed, a statistically greater inhibition of ventral waves was achieved by expression of ASAP1, an Arf1 GAP, as compared to ACAP1, an Arf6 GAP ($P=0.0175$). These differential effects confirm what was observed in Arf1 and Arf6-depleted cells and underscore the primary importance of Arf1 function in mediating changes to cortical actin on the ventral cell surface.

Discussion

Until recently, Arf cellular function has been thought to involve Arfs 1–5 acting at the Golgi complex and Arf6 acting at the cell surface [D'Souza-Schorey and Chavrier 2006; Donaldson and Jackson 2011]. Here we provide evidence for a direct role of a Golgi Arf, Arf1, at the PM, in generating cortical actin structures on the ventral cell surface. Acute treatment of cells with PMA to activate PKC and Src led to the generation of ventral actin structures, and active forms of Arf1 or Arf6 enhanced this process. The collective data suggest that Arf1 and Arf6 can form these structures independently using common effectors but the requirement for Arf1 in forming these structures is notable and was observed in both Beas-2b and HeLa cells. These findings reveal how cell signaling through the activation of PKC and Src can marshal the shared activities of Arf1 and Arf6 to re-organize the cortical actin cytoskeleton.

PKC and Src activity are required for induction of the ventral actin structures. Src is not sufficient to form these structures because expression of an activated mutant of Src in HeLa and Beas-2b cells did not generate the phenotype (unpublished observations) indicating perhaps an additional function for PKC in this process. We think that PKC and Src activation are responsible for altering the actin organization in cells that have sufficient levels of active Arf1 or Arf6. It is especially striking how PMA treatment re-positions and re-purposes Arf1Q71L and Arf6Q67L. Expression of Arf1Q71L leads to the assembly of stable Golgi-associated coated vesicles [Teal et al. 1994] while Arf6Q67L leads to the accumulation of actin-coated endosomal vacuoles [Aikawa and Martin 2003; Brown et al. 2001]. PMA, and therefore PKC and Src activation, re-orient these activated Arfs and bring them to the ventral surface to initiate acute formation of these structures.

The use of the two cell lines in this study helped us define the requirements and role for Arf1 in this process. The Beas-2b cells formed these structures directly in response to PMA treatment but this was inhibited when Arf1 levels were depleted. The HeLa cells, in contrast, did not form the structures unless active forms of Arf1 or Arf6, or specific Arf GEFs were expressed. EFA6 is a BFA-resistant GEF that localizes to the cell surface [Macia et al. 2008] and efficiently activates Arf6 [Franco et al. 1999] but can, to some extent, activate Arf1 [Cohen et al. 2007; Macia et al. 2001]. Consistent with earlier work demonstrating a role for ARNO in relocalizing actin to the edge of HeLa cells upon PMA stimulation [Frank et al. 1998], we also found effects of expression of ARNO in both cell types. However, it is the expression of ARNO-2G that efficiently promotes the formation of these ventral actin structures whereas ARNO-3G does so poorly. Given that ARNO family GEFs are mostly cytoplasmic [Casanova 2007], it would appear that PIP_3 is required for ARNO to support this activity.

Although the requirements for forming ventral actin structures were identical for Beas-2b and HeLa cells, the structures took on different forms. In HeLa cells the ventral structures took the form of ventral ruffles as folds of membrane were present. By contrast, in the Beas-2b cells, the structures lacked a folded membrane component and thus appeared to be more like ventral actin waves, similar to those reported by others [Bretschneider et al. 2004; Case and Waterman 2011; Wu et al. 2013]. The ventral actin events are clearly distinct from dorsal ruffles generated in response to growth factor signaling, which are dependent upon Arf1 and Arf5 and ARAP1, an Arf GAP [Hasegawa et al. 2012]. Indeed, in the Beas-2b cells it is notable that these actin waves appear to form at focal adhesions, sites where Src and the Arf1 GAP ASAP are present.

Several studies have implicated Arf1 in playing a direct role in rearrangements of cortical actin. Arf1 can cooperate with Rac1 to promote actin polymerization in vitro [Koronakis et al. 2011] and they appear to be involved in cell migration in an invasive breast cancer cell line [Lewis-Saravalli et al. 2013]. Arf1 through its interaction with Pick1 was shown to regulate actin turnover in dendritic spines [Rocca et al. 2013]. Furthermore, the Arf1 homologue in Drosophila has been shown to be important for the formation of lamellipodium by recruiting the WAVE regulatory complex to the plasma membrane [Humphreys et al. 2012]. At the cell surface, Arf1 could be organizing actin in a manner similar to its ability to organize actin at the Golgi by engaging pools of actin associated with

cortactin or drebrin [Cao et al. 2005; Fucini et al. 2000]. Indeed both cortactin and drebrin are associated with the ventral structures observed here (Supporting Information Fig. S5 and unpublished observations). Additionally, human Arf1 can recruit ARHGAP10, a GAP for Cdc42 [Dubois et al. 2005], which may relate to roles for Cdc42 that have been reported in formation of podosomes and invadopodia in some cells [Albiges-Rizo et al. 2009]. Arf1 could also be engaging its GAP, ASAP1 at these sites; consistent with this notion, actin wave formation was inhibited in Beas-2b cells upon over-expression of ASAP1. ASAP1 localizes to focal adhesions [Brown et al. 1998] and promotes invadopodia formation [Bharti et al. 2007]. Since Arf1 and Arf6 share many common effectors, including PIP5-kinase and PLD, the acute recruitment of additional Arf (Arf1) at the site where ventral actin structures form might augment Arf6 function. Thus PMA treatment of HeLa or Beas-2b cells reveals a new activity for Arf1 at the PM reorganizing cortical actin at ventral surfaces. Nonetheless, we cannot rule out a critical role for Arf6 in this process.

Present at the cell surface, Arf6 is poised to participate in the formation of PMA-induced ventral ruffles, which is not surprising based on the literature linking Arf6 to changes in cell surface architecture [D'Souza-Schorey and Chavrier 2006]. The ventral actin waves and ruffles that we observed in Beas-2b and HeLa cells resemble classic v-src-induced podosomes formed in NIH 3T3 cells and the PMA-induced structures in various cell lines [Block et al. 2008]. Arf6 is involved in podosome formation in dendritic cells [Svensson et al. 2008], invasive capacity in melanoma [Tague et al. 2004] and glioma cells [Hu et al. 2009], and invasion, degradation and migration of breast cancer cells [Hashimoto et al. 2004]. Whether the ventral actin events observed here are precursors of some of these other activities remains to be determined. The fact that Arf1 contributes to the formation of ventral actin structures that we observed also suggests that Arf1 may act in some of these other invasion and migration activities as well.

The interplay between PMA-activated Src and PKC, and active Arf proteins suggests two parallel but independent pathways that converge to create ventral actin structures, a profound change in cell surface architecture. Activation of Arf1 in the periphery in combination with activation of PKC and Src may be important in switching a cell from focal adhesion based adhesion with peripheral protrusions to podosome based adhesion with ventral ruffles or waves. Exactly how Arf1 can spatially redirect actin polymerization to the ventral cell surface and the role that membrane traffic plays in this restructuring will require further investigation.

Materials and Methods

Plasmids, Antibodies, and other reagents

FLAG-tagged EFA6 encodes the shorter form of human EFA6A is as described [Brown et al. 2001]. FLAG-tagged ARNO 3G was from Jim Casanova (University of Virginia, Charlottesville, VA.); the 2G variant was produced by site directed mutagenesis. Plasmids for untagged, human Arf6, Arf6T27N, and Arf6Q67L were in pxs vector as described [Brown et al. 2001]. The plasmids for Arf1 and Arf1Q71L were in pEGFP and encode human Arf1 with a GFP or RFP tag fused to their carboxyl termini. Arf1T31N-HA was in pxs vector. Rac1Q71L and Rac1T31N are untagged. Myc-tagged p72 5-phosphatase was

from Tamas Balla (NIH). Myc tagged PIP 5-kinase type I α (PIP5-kinase) was previous described [Rozelle et al. 2000]. GFP-Actin is in pEGFP and encodes actin with a GFP appended to its amino terminus was from Jennifer Lippincott-Schwartz (NIH). LifeAct-RFP, a 17 amino acid peptide that binds to filamentous actin [Riedl et al. 2008], was from Roberto Weigert (NIDCR). Mem-GFP encodes GFP fused to the carboxyl terminal tail of H-Ras and was purchased from Clontech (Mountain View, CA). Plasmids encoding Flag-ASAP1, Flag-ASAP1 RK, Flag-ACAP1 and Flag-ACAP1 RQ were as described [Jackson et al. 2000].

The following antibodies were used in this study. The M2 mouse anti-FLAG and rabbit anti-FLAG antibodies were from Sigma. A rabbit polyclonal antibody was used to detect Arf6 [Song et al. 1998]. A rabbit polyclonal antibody against human Arf1 carboxyl terminal amino acids 168–181 was generated. Mouse monoclonal anti-Arf6 (3A-1) and anti-myc epitope (9E10) antibodies were from Santa Cruz Biotechnology. A rabbit polyclonal anti-GFP antibody was from Invitrogen. A mouse monoclonal antibody to HA (16b12) was from Covance. Mouse monoclonal antibody to GM130 was from Transduction Labs. Monoclonal antibodies to Rac1 and cortactin (4F11) were from Millipore. The rabbit polyclonal antibody against beta subunit of COP I was from Thermo Fisher. Phospho-paxillin and phospho-FAK were detected with phosphospecific rabbit polyclonal antibodies anti-paxillin PY31 and anti-FAK Y397 respectively, both from Biosource, Camarillo, CA. Alexa-conjugated (488 ,594, and 680) goat anti-mouse and goat anti-rabbit antibodies and Rhodamine phalloidin and Alexa fluor 633-conjugated phalloidin were from Invitrogen and used according to manufacturer's instructions.

Phorbol 12-myristate 13-acetate (PMA) and Brefeldin A (BFA) were from Sigma. GF 109203x, PP2, and PP3 were from EMD4Biosciences. All stock solutions were made up in DMSO and stored according to manufacturer's instructions.

Cell Culture and Transient Transfections

HeLa cells were maintained in DMEM supplemented with 10% fetal bovine serum (FBS), 100 U/ml penicillin, and 100 μg/ml streptomycin at 37°C with 5% CO_2. Beas-2b cells were obtained from ATCC, and maintained in low glucose (1g/L) DMEM supplemented with 10% fetal bovine serum (FBS), 100 U/ml penicillin, and 100 μg/ml streptomycin at 37°C with 5% CO_2. For transient transfections, cells were plated the day before and then transfected the following day with Fugene 6 according to the manufacturer's instructions. Experiments were carried out as described ~18 h after DNA addition.

Immunofluorescent Staining and Live Cell Imaging

For immunofluorescence staining of HeLa or Beas-2b cells, cells were plated on to glass coverslips and transfected on the following day. Eighteen hours after transfection, cells were treated as described and then fixed in 2% formaldehyde in phosphate buffered saline (PBS) for 10 min. Cells were washed in PBS supplemented with 10% FBS (PBS/FBS) and incubated with primary antibodies diluted in PBS/FBS containing 0.2% saponin for 1 h. Cells were washed three times in PBS/FBS and incubated with the appropriate secondary antibodies in PBS/FBS containing 0.2% saponin for 30 min. Cells were washed three times in PBS/FBS, once in PBS alone and then mounted on glass slides. All experiments were

confirmed by at least three independent experiments, and a representative image is shown. Where indicated, ventral ruffles or waves were quantified from immunofluorescence experiments by counting 100 cells and scoring the number that had 1 or more clear ventral actin structures visible by phalloidin staining. For Figures 1, 2, 4, and 6, data is presented as the average percentage of cells with ventral actin structures from 3 independent experiments with error bars representing 1 standard deviation. ANOVA, T-test and Tukey multiple comparison statistical tests were used. In Figures 3, 7 and Supplemental Figure S6, the data represents the proportion of the total amount of cells counted, and error bars represent standard error for binomial distribution: $\sqrt{p(1-p)/n}$, where p is the proportion and n is the total number of cells assessed. Statistical significance was assessed by calculating P-values using Fisher's Exact test (two-tailed.)

Images were taken using a Zeiss 510 laser scanning confocal microscope (Thornwood, NY) using a 63x 1.3 NA PlanApo objective. After acquisition, images were handled using AdobePhotoshop (San Jose, CA).

For live cell imaging, HeLa or Beas-2b cells were plated in Lab-Tek coverglass chambers (Nunc, Rochester NY). On the following day they were transfected with the indicated constructs. Cells were imaged approximately 18 h after transfection on a 37°C stage with 5% CO_2 maintained by a CO_2 chamber. Cells expressing low to moderate levels of GFP-Actin were chosen for imaging as higher levels of expression of this construct tended to inhibit the processes being studied. Three or more cells were imaged for each experiment, and a representative movie is shown. Images were captured on a Zeiss LSM 780 confocal microscope with a 63x/NA 1.4 PlanApo objective. Movies were compiled using MetaMorph (Molecular Devices, Natick, MA). Movies presented in supplemental material are compiled at a frame rate of 10 frames/sec. Frames were taken 30 seconds apart.

Transfection with siRNA

The day prior to transfection with siRNA 2.0×10^5 Beas-2b cells were plated into antibiotic-free media in a 100 mm tissue culture dish. The following day cells were incubated with Lipofectamine 2000 (Invitrogen, Carlsbad CA) containing the specific siRNA sequence according to manufacturers instructions. Cells were placed into fresh media after 3 h, and grown in culture for 72 h. Experiments were conducted as described. The remaining cells were collected and 5 X 10^5 cells were used for immunoblotting to confirm the extent of knockdown. For siRNA of Arf1 or Arf6 in HeLa cells, siRNA oligos, Lipofectamine RNAiMax (Invitrogen, Carlsbad CA) and 1.0×10^4 cells were combined in each well of a 12-well plate in accordance with manufacturer specifications for a reverse transfection. After 48 hours, the cells were transfected with EFA6-Flag and 24 hours later, the cells on coverslips were fixed and evaluated by immunocytochemistry and remaining cells were collected for western blotting.

For Arf1 knockdown we used ON-TARGETplus Smart pool of four combined sequences purchased from (Dharmacon Lafayatte, CO). 60nM of pooled oligo was used for Arf1 knockdown in Beas-2b cells and 10nM of pooled oligo was used for knockdown of Arf1 in HeLa cells. For Arf6 knockdown, we used siRNA oligo with the sequence GCA CCG CAU

UAU CAA UGA CCG manufactured by Dharmacon (Lafayette, CO) and previously described for knockdown of Arf6 in other systems [Hashimoto et al. 2004]. 20nM was used for Arf6 knockdown in Beas-2b cells and 100nM was used for knockdown of Arf6 in HeLa cells. Although we initially used scrambled sequences for control siRNA, we found the results to be the same as that observed for Lipofectamine alone and thus used Lipofectamine alone for control cells.

Arf detection by Immunoblot

5 X 10^5 cells were collected and lysed in 1% triton X-100, 10% glycerol, 100 mM NaCl, and 50 mM Tris pH 7.4. Lysates were cleared by centrifugation. The resulting supernatant was diluted in 5x SDS PAGE sample buffer and boiled. Lysates were resolved by SDS PAGE, followed by transfer to nitrocellulose membrane. Western blots were carried out using a rabbit polyclonal antibody to Arf1, a rabbit polyclonal antibody to Arf6 (see details above) or a mouse monoclonal antibody to Arf6 (Santa Cruz Biotechnology), and a rabbit antibody to actin (Sigma), and a mouse monoclonal antibody to α-tubulin (DM1A) (Sigma). The primary antibodies were detected with Alexa 680-conjugated donkey anti-sheep, IR dye 800-conjugated donkey anti-mouse and donkey anti-rabbit (Rockland Immunochemicals). Blots were visualized using an Odyssey infrared scanner (Li-Cor Bioscience) according to manufacturer's instructions.

Supplementary Material

Refer to Web version on PubMed Central for supplementary material.

Acknowledgments

We thank members of the Donaldson lab for discussion and comments on the manuscript. Microscopes used in this study are part of the NHLBI Light Microscopy Facility. This work was supported by the Intramural Research Program in the National Heart, Lung, and Blood Institute (HL000517). All authors declare that we have no conflict of interest in the publication of this material.

Abbreviations

GAP	GTPase activating protein
GEF	guanine nucleotide exchange factor
PIP_2	phosphatidylinositol 4,5-bisphosphate
PIP_3	phosphatidylinositol 3,4,5-trisphosphate
PIP5-kinase	phosphatidylinositol 4-phosphate 5-kinase
PKC	protein kinase C
PLD	phospholipase D
PMA	phorbol 12-myristate 13-acetate

References

Aikawa Y, Martin TFJ. ARF6 regulates a plasma membrane pool of phosphatidylinositol(4,5)bisphosphate required for regulated exocytosis. J Cell Biol. 2003; 162(4): 647–659. [PubMed: 12925709]

Albiges-Rizo C, Destaing O, Fourcade B, Planus E, Block MR. Actin machinery and mechanosensitivity in invadopodia, podosomes and focal adhesions. J Cell Sci. 2009; 122(Pt 17): 3037–49. [PubMed: 19692590]

Balasubramanian N, Scott DW, Castle JD, Casanova JE, Schwartz MA. Arf6 and microtubules in adhesion-dependent trafficking of lipid rafts. Nat Cell Biol. 2007; 9(12):1381–91. [PubMed: 18026091]

Beemiller P, Hoppe AD, Swanson JA. A phosphatidylinositol-3-kinase-dependent signal transition regulates ARF1 and ARF6 during Fcgamma receptor-mediated phagocytosis. PLoS Biol. 2006; 4(6):e162. [PubMed: 16669702]

Bharti S, Inoue H, Bharti K, Hirsch DS, Nie Z, Yoon HY, Artym V, Yamada KM, Mueller SC, Barr VA, et al. Src-dependent phosphorylation of ASAP1 regulates podosomes. Mol Cell Biol. 2007; 27(23):8271–83. [PubMed: 17893324]

Block MR, Badowski C, Millon-Fremillon A, Bouvard D, Bouin AP, Faurobert E, Gerber-Scokaert D, Planus E, Albiges-Rizo C. Podosome-type adhesions and focal adhesions, so alike yet so different. Eur J Cell Biol. 2008; 87(8–9):491–506. [PubMed: 18417250]

Boshans RL, Szanto S, van Aelst L, D'Souza-Schorey C. ADP-ribosylation factor 6 regulates actin cytoskeleton remodeling in coordination with Rac1 and RhoA. Mol Cell Biol. 2000; 20(10):3685–94. [PubMed: 10779358]

Boulay PL, Cotton M, Melancon P, Claing A. ADP-ribosylation factor 1 controls the activation of the phosphatidylinositol 3-kinase pathway to regulate epidermal growth factor-dependent growth and migration of breast cancer cells. J Biol Chem. 2008; 283(52):36425–34. [PubMed: 18990689]

Brandt DT, Goerke A, Heuer M, Gimona M, Leitges M, Kremmer E, Lammers R, Haller H, Mischak H. Protein kinase C delta induces Src kinase activity via activation of the protein tyrosine phosphatase PTP alpha. The Journal of biological chemistry. 2003; 278(36):34073–8. [PubMed: 12826681]

Bretschneider T, Diez S, Anderson K, Heuser J, Clarke M, Muller-Taubenberger A, Kohler J, Gerisch G. Dynamic actin patterns and Arp2/3 assembly at the substrate-attached surface of motile cells. Current biology : CB. 2004; 14(1):1–10. [PubMed: 14711408]

Brown FD, Rozelle AL, Yin HL, Balla T, Donaldson JG. Phosphatidylinositol 4,5-bisphosphate and Arf6-regulated membrane traffic. J Cell Biol. 2001; 154(5):1007–17. [PubMed: 11535619]

Brown HA, Gutowski S, Moomaw CR, Slaughter C, Sternweis PC. ADP-ribosylation factor, a small GTP-dependent regulatory protein, stimulates phospholipase D activity. Cell. 1993; 75(6):1137–44. [PubMed: 8261513]

Brown MT, Andrade J, Radhakrishna H, Donaldson JG, Cooper JA, Randazzo PA. ASAP1, a phospholipid-dependent arf GTPase-activating protein that associates with and is phosphorylated by Src. Mol Cell Biol. 1998; 18(12):7038–51. [PubMed: 9819391]

Caldieri G, Buccione R. Aiming for invadopodia: organizing polarized delivery at sites of invasion. Trends in cell biology. 2010; 20(2):64–70. [PubMed: 19931459]

Cao H, Weller S, Orth JD, Chen J, Huang B, Chen JL, Stamnes M, McNiven MA. Actin and Arf1-dependent recruitment of a cortactin-dynamin complex to the Golgi regulates post-Golgi transport. Nat Cell Biol. 2005; 7(5):483–92. [PubMed: 15821732]

Casanova JE. Regulation of Arf activation: the Sec7 family of guanine nucleotide exchange factors. Traffic. 2007; 8(11):1476–85. [PubMed: 17850229]

Case LB, Waterman CM. Adhesive F-actin waves: a novel integrin-mediated adhesion complex coupled to ventral actin polymerization. PLoS One. 2011; 6(11):e26631. [PubMed: 22069459]

Cockcroft S, Thomas GM, Fensome A, Geny B, Cunningham E, Gout I, Hiles I, Totty NF, Truong O, Hsuan JJ. Phospholipase D: a downstream effector of ARF in granulocytes. Science. 1994; 263(5146):523–6. [PubMed: 8290961]

Cohen LA, Honda A, Varnai P, Brown FD, Balla T, Donaldson JG. Active Arf6 recruits ARNO/cytohesin GEFs to the PM by binding their PH domains. Mol Biol Cell. 2007; 18(6):2244–53. [PubMed: 17409355]

D'Souza-Schorey C, Chavrier P. ARF proteins: roles in membrane traffic and beyond. Nat Rev Mol Cell Biol. 2006; 7(5):347–58. [PubMed: 16633337]

Daher Z, Boulay PL, Desjardins F, Gratton JP, Claing A. Vascular endothelial growth factor receptor-2 activates ADP-ribosylation factor 1 to promote endothelial nitric-oxide synthase activation and nitric oxide release from endothelial cells. J Biol Chem. 2010; 285(32):24591–9. [PubMed: 20529868]

Dascher C, Balch WE. Dominant inhibitory mutants of ARF1 block endoplasmic reticulum to Golgi transport and trigger disassembly of the Golgi apparatus. J Biol Chem. 1994; 269(2):1437–48. [PubMed: 8288610]

Donaldson JG, Honda A, Weigert R. Multiple activities for Arf1 at the Golgi complex. Biochim Biophys Acta. 2005; 1744(3):364–73. [PubMed: 15979507]

Donaldson JG, Jackson CL. ARF family G proteins and their regulators: roles in membrane transport, development and disease. Nature reviews Molecular cell biology. 2011; 12(6):362–75. [PubMed: 21587297]

Donaldson JG, Porat-Shliom N, Cohen LA. Clathrin-independent endocytosis: a unique platform for cell signaling and PM remodeling. Cell Signal. 2009; 21(1):1–6. [PubMed: 18647649]

Dubois T, Paleotti O, Mironov AA, Fraisier V, Stradal TE, De Matteis MA, Franco M, Chavrier P. Golgi-localized GAP for Cdc42 functions downstream of ARF1 to control Arp2/3 complex and F-actin dynamics. Nature cell biology. 2005; 7(4):353–64. [PubMed: 15793564]

Eyster CA, Higginson JD, Huebner R, Porat-Shliom N, Weigert R, Wu WW, Shen RF, Donaldson JG. Discovery of New Cargo Proteins that Enter Cells through Clathrin-Independent Endocytosis. Traffic. 2009; 10(5):590–599. [PubMed: 19302270]

Franco M, Peters PJ, Boretto J, van Donselaar E, Neri A, D'Souza-Schorey C, Chavrier P. EFA6, a sec7 domain-containing exchange factor for ARF6, coordinates membrane recycling and actin cytoskeleton organization. Embo J. 1999; 18(6):1480–91. [PubMed: 10075920]

Frank SR, Hatfield JC, Casanova JE. Remodeling of the actin cytoskeleton is coordinately regulated by protein kinase C and the ADP-ribosylation factor nucleotide exchange factor ARNO. Mol Biol Cell. 1998; 9(11):3133–46. [PubMed: 9802902]

Fucini RV, Navarrete A, Vadakkan C, Lacomis L, Erdjument-Bromage H, Tempst P, Stamnes M. Activated ADP-ribosylation factor assembles distinct pools of actin on golgi membranes. J Biol Chem. 2000; 275(25):18824–9. [PubMed: 10777475]

Gavazzi I, Nermut MV, Marchisio PC. Ultrastructure and gold-immunolabelling of cell-substratum adhesions (podosomes) in RSV-transformed BHK cells. J Cell Sci. 1989; 94(Pt 1):85–99. [PubMed: 2482298]

Godi A, Pertile P, Meyers R, Marra P, Di Tullio G, Iurisci C, Luini A, Corda D, De Matteis MA. ARF mediates recruitment of PtdIns-4-OH kinase-beta and stimulates synthesis of PtdIns(4,5)P2 on the Golgi complex. Nature cell biology. 1999; 1(5):280–7. [PubMed: 10559940]

Grant BD, Donaldson JG. Pathways and mechanisms of endocytic recycling. Nat Rev Mol Cell Biol. 2009; 10(9):597–608. [PubMed: 19696797]

Hasegawa J, Tsujita K, Takenawa T, Itoh T. ARAP1 regulates the ring size of circular dorsal ruffles through Arf1 and Arf5. Molecular biology of the cell. 2012; 23(13):2481–9. [PubMed: 22573888]

Hashimoto S, Onodera Y, Hashimoto A, Tanaka M, Hamaguchi M, Yamada A, Sabe H. Requirement for Arf6 in breast cancer invasive activities. Proc Natl Acad Sci U S A. 2004; 101(17):6647–52. [PubMed: 15087504]

Heasman SJ, Ridley AJ. Mammalian Rho GTPases: new insights into their functions from in vivo studies. Nat Rev Mol Cell Biol. 2008; 9(9):690–701. [PubMed: 18719708]

Hernandez-Deviez DJ, Casanova JE, Wilson JM. Regulation of dendritic development by the ARF exchange factor ARNO. Nat Neurosci. 2002; 5(7):623–4. [PubMed: 12032543]

Hernandez-Deviez DJ, Roth MG, Casanova JE, Wilson JM. ARNO and ARF6 Regulate Axonal Elongation and Branching through Downstream Activation of Phosphatidylinositol 4-Phosphate 5-Kinase {alpha}. Mol Biol Cell. 2004; 15(1):111–120. [PubMed: 14565977]

Honda A, Nogami M, Yokozeki T, Yamazaki M, Nakamura H, Watanabe H, Kawamoto K, Nakayama K, Morris AJ, Frohman MA, et al. Phosphatidylinositol 4-phosphate 5-kinase alpha is a downstream effector of the small G protein ARF6 in membrane ruffle formation. Cell. 1999; 99(5):521–32. [PubMed: 10589680]

Hu B, Shi B, Jarzynka MJ, Yiin JJ, D'Souza-Schorey C, Cheng SY. ADP-ribosylation factor 6 regulates glioma cell invasion through the IQ-domain GTPase-activating protein 1-Rac1-mediated pathway. Cancer Res. 2009; 69(3):794–801. [PubMed: 19155310]

Humphreys D, Liu T, Davidson AC, Hume PJ, Koronakis V. The Drosophila Arf1 homologue Arf79F is essential for lamellipodium formation. Journal of cell science. 2012; 125(Pt 23):5630–5. [PubMed: 22992458]

Jackson TR, Brown FD, Nie Z, Miura K, Foroni L, Sun J, Hsu VW, Donaldson JG, Randazzo PA. ACAPs are arf6 GTPase-activating proteins that function in the cell periphery. J Cell Biol. 2000; 151(3):627–38. [PubMed: 11062263]

Jovanovic OA, Brown FD, Donaldson JG. An effector domain mutant of Arf6 implicates phospholipase D in endosomal membrane recycling. Mol Biol Cell. 2006; 17(1):327–35. [PubMed: 16280360]

Klarlund JK, Tsiaras W, Holik JJ, Chawla A, Czech MP. Distinct polyphosphoinositide binding selectivities for pleckstrin homology domains of GRP1-like proteins based on diglycine versus triglycine motifs. J Biol Chem. 2000; 275(42):32816–21. [PubMed: 10913124]

Koo TH, Eipper BA, Donaldson JG. Arf6 recruits the Rac GEF Kalirin to the plasma membrane facilitating Rac activation. BMC Cell Biol. 2007; 8:29. [PubMed: 17640372]

Koronakis V, Hume PJ, Humphreys D, Liu T, Horning O, Jensen ON, McGhie EJ. WAVE regulatory complex activation by cooperating GTPases Arf and Rac1. Proceedings of the National Academy of Sciences of the United States of America. 2011; 108(35):14449–54. [PubMed: 21844371]

Ktistakis NT, Brown HA, Sternweis PC, Roth MG. Phospholipase D is present on Golgi-enriched membranes and its activation by ADP ribosylation factor is sensitive to brefeldin A. Proc Natl Acad Sci U S A. 1995; 92(11):4952–6. [PubMed: 7761430]

Kumari S, Mayor S. ARF1 is directly involved in dynamin-independent endocytosis. Nat Cell Biol. 2008; 10(1):30–41. [PubMed: 18084285]

Lewis-Saravalli S, Campbell S, Claing A. ARF1 controls Rac1 signaling to regulate migration of MDA-MB-231 invasive breast cancer cells. Cellular signalling. 2013; 25(9):1813–9. [PubMed: 23707487]

Liu Y, Loijens JC, Martin KH, Karginov AV, Parsons JT. The association of ASAP1, an ADP ribosylation factor-GTPase activating protein, with focal adhesion kinase contributes to the process of focal adhesion assembly. Molecular biology of the cell. 2002; 13(6):2147–56. [PubMed: 12058076]

Macia E, Chabre M, Franco M. Specificities for the small G proteins ARF1 and ARF6 of the guanine nucleotide exchange factors ARNO and EFA6. J Biol Chem. 2001; 276(27):24925–30. [PubMed: 11342560]

Macia E, Partisani M, Favard C, Mortier E, Zimmermann P, Carlier MF, Gounon P, Luton F, Franco M. The pleckstrin homology domain of the Arf6-specific exchange factor EFA6 localizes to the plasma membrane by interacting with phosphatidylinositol 4,5-bisphosphate and F-actin. The Journal of biological chemistry. 2008; 283(28):19836–44. [PubMed: 18490450]

Palacios F, Price L, Schweitzer J, Collard JG, D'Souza-Schorey C. An essential role for ARF6-regulated membrane traffic in adherens junction turnover and epithelial cell migration. Embo J. 2001; 20(17):4973–86. [PubMed: 11532961]

Porat-Shliom N, Kloog Y, Donaldson JG. A Unique Platform for H-Ras Signaling Involving Clathrin-independent Endocytosis. Mol Biol Cell. 2008; 19(3):765–75. [PubMed: 18094044]

Powelka AM, Sun J, Li J, Gao M, Shaw LM, Sonnenberg A, Hsu VW. Stimulation-dependent recycling of integrin beta1 regulated by ARF6 and Rab11. Traffic. 2004; 5(1):20–36. [PubMed: 14675422]

Riedl J, Crevenna AH, Kessenbrock K, Yu JH, Neukirchen D, Bista M, Bradke F, Jenne D, Holak TA, Werb Z, et al. Lifeact: a versatile marker to visualize F-actin. Nat Methods. 2008; 5(7):605–7. [PubMed: 18536722]

Rocca DL, Amici M, Antoniou A, Suarez EB, Halemani N, Murk K, McGarvey J, Jaafari N, Mellor JR, Collingridge GL, et al. The small GTPase Arf1 modulates Arp2/3-mediated actin polymerization via PICK1 to regulate synaptic plasticity. Neuron. 2013; 79(2):293–307. [PubMed: 23889934]

Rozelle AL, Machesky LM, Yamamoto M, Driessens MH, Insall RH, Roth MG, Luby-Phelps K, Marriott G, Hall A, Yin HL. Phosphatidylinositol 4,5-bisphosphate induces actin-based movement of raft-enriched vesicles through WASP-Arp2/3. Curr Biol. 2000; 10(6):311–20. [PubMed: 10744973]

Sabe H, Hashimoto S, Morishige M, Ogawa E, Hashimoto A, Nam JM, Miura K, Yano H, Onodera Y. The EGFR-GEP100-Arf6-AMAP1 signaling pathway specific to breast cancer invasion and metastasis. Traffic. 2009; 10(8):982–93. [PubMed: 19416474]

Santy LC, Casanova JE. Activation of ARF6 by ARNO stimulates epithelial cell migration through downstream activation of both Rac1 and phospholipase D. J Cell Biol. 2001; 154(3):599–610. [PubMed: 11481345]

Santy LC, Frank SR, Casanova JE. Expression and analysis of ARNO and ARNO mutants and their effects on ADP-ribosylation factor (ARF)-mediated actin cytoskeletal rearrangements. Methods Enzymol. 2001; 329:256–64. [PubMed: 11210542]

Santy LC, Ravichandran KS, Casanova JE. The DOCK180/Elmo complex couples ARNO-mediated Arf6 activation to the downstream activation of Rac1. Curr Biol. 2005; 15(19):1749–54. [PubMed: 16213822]

Schafer DA, D'Souza-Schorey C, Cooper JA. Actin assembly at membranes controlled by ARF6. Traffic. 2000; 1(11):892–903. [PubMed: 11273133]

Song J, Khachikian Z, Radhakrishna H, Donaldson JG. Localization of endogenous ARF6 to sites of cortical actin rearrangement and involvement of ARF6 in cell spreading. J Cell Sci. 1998; 111(Pt 15):2257–67. [PubMed: 9664047]

Svensson HG, West MA, Mollahan P, Prescott AR, Zaru R, Watts C. A role for ARF6 in dendritic cell podosome formation and migration. Eur J Immunol. 2008; 38(3):818–28. [PubMed: 18286566]

Tague SE, Muralidharan V, D'Souza-Schorey C. ADP-ribosylation factor 6 regulates tumor cell invasion through the activation of the MEK/ERK signaling pathway. Proc Natl Acad Sci U S A. 2004; 101(26):9671–6. [PubMed: 15210957]

Tatin F, Varon C, Genot E, Moreau V. A signalling cascade involving PKC, Src and Cdc42 regulates podosome assembly in cultured endothelial cells in response to phorbol ester. J Cell Sci. 2006; 119(Pt 4):769–81. [PubMed: 16449321]

Teal SB, Hsu VW, Peters PJ, Klausner RD, Donaldson JG. An activating mutation in ARF1 stabilizes coatomer binding to Golgi membranes. J Biol Chem. 1994; 269(5):3135–8. [PubMed: 8106346]

Volpicelli-Daley LA, Li Y, Zhang CJ, Kahn RA. Isoform-selective effects of the depletion of ADP-ribosylation factors 1–5 on membrane traffic. Mol Biol Cell. 2005; 16(10):4495–508. [PubMed: 16030262]

Whatmore J, Morgan CP, Cunningham E, Collison KS, Willison KR, Cockcroft S. ADP-ribosylation factor 1-regulated phospholipase D activity is localized at the plasma membrane and intracellular organelles in HL60 cells. Biochem J. 1996; 320(Pt 3):785–94. [PubMed: 9003363]

Wu M, Wu X, De Camilli P. Calcium oscillations-coupled conversion of actin travelling waves to standing oscillations. Proceedings of the National Academy of Sciences of the United States of America. 2013; 110(4):1339–44. [PubMed: 23297209]

Xiao H, Bai XH, Kapus A, Lu WY, Mak AS, Liu M. PKC cascade regulates recruitment of MMP-9 to podosomes and its release and activation. Mol Cell Biol. 2010

Xiao H, Eves R, Yeh C, Kan W, Xu F, Mak AS, Liu M. Phorbol ester-induced podosomes in normal human bronchial epithelial cells. J Cell Physiol. 2009; 218(2):366–75. [PubMed: 18932175]

Zimmermann P, Zhang Z, Degeest G, Mortier E, Leenaerts I, Coomans C, Schulz J, N'Kuli F, Courtoy PJ, David G. Syndecan recycling is controlled by syntenin-PIP2 interaction and Arf6. Dev Cell. 2005; 9(3):377–88. [PubMed: 16139226]

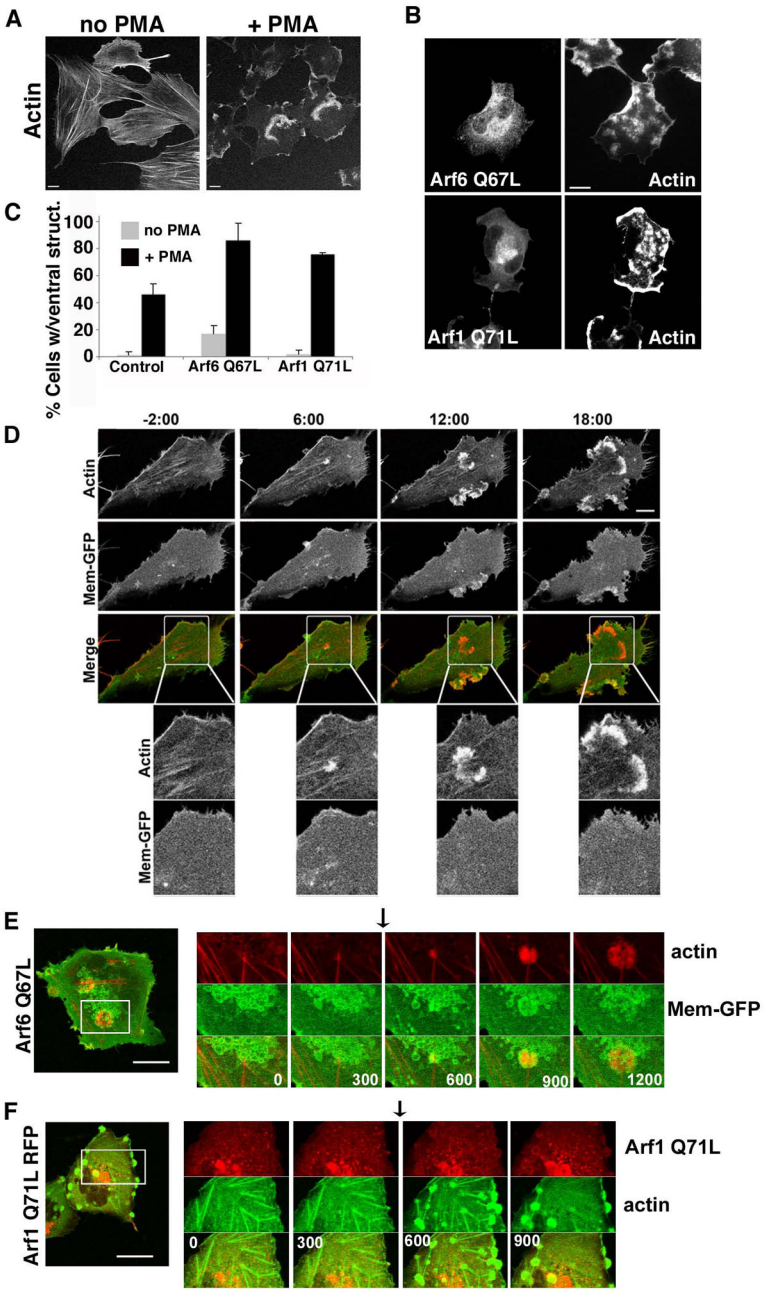

Figure 1. PMA treated Beas-2b cells form ventral actin waves

(A) Untransfected Beas-2b cells were treated with vehicle (no PMA) or 200 nM PMA for 30 min prior to fixation and staining with rhodamine phalloidin. (B) Beas-2b cells were transfected with plasmids encoding untagged Arf6 Q67L (top) or Arf1 Q71L-GFP (bottom) and treated with 200 nM PMA for 30 min prior to fixation and labeling with antibodies to Arf6 for Arf6 detection and actin. Bars, 10 μm. (C) The fraction of transfected cells with 1 or more ventral waves was quantified and is expressed as the average percentage obtained from three independent experiments. Error bars represent standard deviation from the means. GFP was used as a control for transfection. One-way ANOVA test of the PMA-

treated Control vs. Arf6Q67L- and Arf1Q71L-transfected cells were significant ($p<0.05$). (D) Beas-2b cells transfected with Mem-GFP and RFP-LifeAct were imaged as described in Materials and Methods. PMA was added after 2 min, designated time 0, and frames were captured every 30 seconds thereafter. Selected stills from the movie at −2, 6,12 and 18 min are shown (see Movie 1 in Supplementary materials). No membrane folds are associated with actin structures. Bar, 10μM. Boxed regions are shown at higher magnification below each time point. Bar, 5μM. (E) Beas-2b cells were transfected with plasmids encoding untagged Arf6 Q67L (in background), Mem-GFP to mark vacuolar membranes in transfected cells, and LifeAct-RFP (to visualize actin). A cell was imaged for 20 min; at 5 min, 200 nM PMA was added (arrow) to induce ventral wave formation (Movie 2 in Supplementary materials). (F) Beas-2b cells were transfected with plasmids encoding Arf1-Q71L-RFP and GFP-Actin. A cell was imaged for 15 minutes; at 5 min 200 nM PMA was added (arrow) to induce ventral wave formation (Movie 3 in Supplementary materials). Shown for each movie is an image of the entire cell taken at the end of the movie with a square around the region shown in the movie. A series of frames from the movie with time indicated in seconds from the beginning of the movie is also shown. Black arrows indicate when PMA was added. Bars,10 μm.

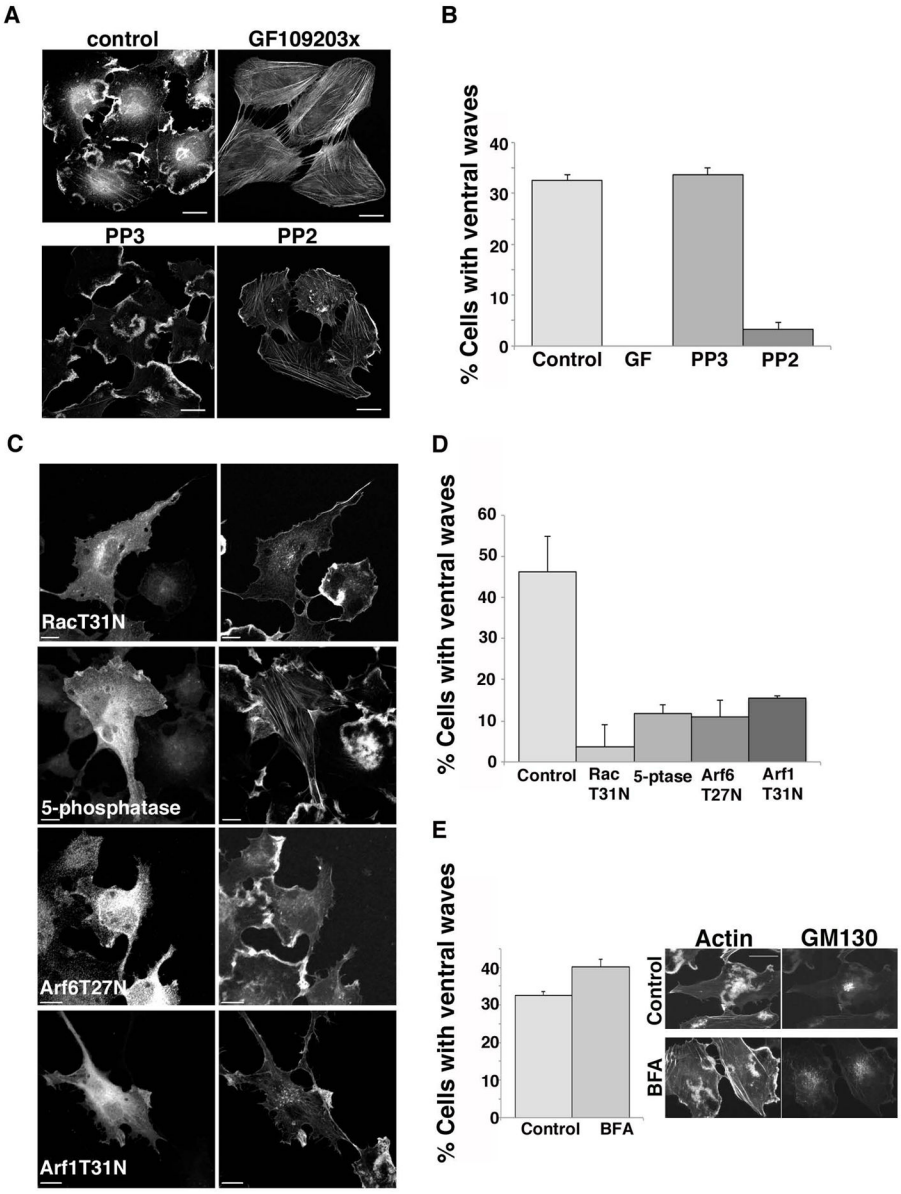

Figure 2. Ventral actin wave formation in Beas-2b cells requires PKC, Src, Rac activity, PIP_2, and Arf

(A) Beas-2b cells were treated for 30 min with 200 nM PMA in the absence or presence of 10 μM GF 109303x (inhibitor of PKC), 10 μM PP3 (inactive analog of PP2) or 10 μM PP2 (inhibitor of Src) as indicated. Following PMA treatment, cells were fixed and stained with rhodamine phalloidin as described. Bars,10 μm. (B) Fraction of control or drug-treated cells with 1 or more ventral waves visible in phalloidin stain was quantified and is expressed as the average percentage from three independent experiments. Error bars represent standard deviation from the mean. Tukey multiple comparison test showed that GF and PP2 differed from the Control ($p<0.001$). **(C)** Beas-2b cells expressing untagged Rac T31N, the p72 $PI(4,5)P_2$ 5-phosphatase (myc tagged), Arf6 T27N, or Arf1 T31N-HA were treated with 200 nM PMA 30 min prior to fixation and immunofluorescence staining as described in the

Material and Methods section with an appropriate primary antibody to detect the transfected protein and Alexa 488 conjugated secondary antibody. Cells were co-stained with rhodamine phalloidin (right panels). (D) Fraction of transfected cells with 1 or more ventral waves visible in phalloidin stain was quantified and is expressed as the average percentage from three independent experiments. Error bars represent standard deviation from the mean. One way ANOVA test showed all treatments differed from Control ($p<0.001$). (E) Untransfected Beas-2b cells were left untreated (control) or pretreated for 2 h with 5 μg/ml brefeldin A (BFA). Both sets of cells were treated with 200 nM PMA for 30 min prior to fixation and staining with rhodamine phalloidin and antibody to GM130. The percentage of cells with 1 or more ventral waves was quantified and is expressed as the average percentage of three independent experiments. Error bars represent one standard deviation from the mean. Student's T-test showed Control vs. BFA treated was not statistically significant. Bars,10 μm.

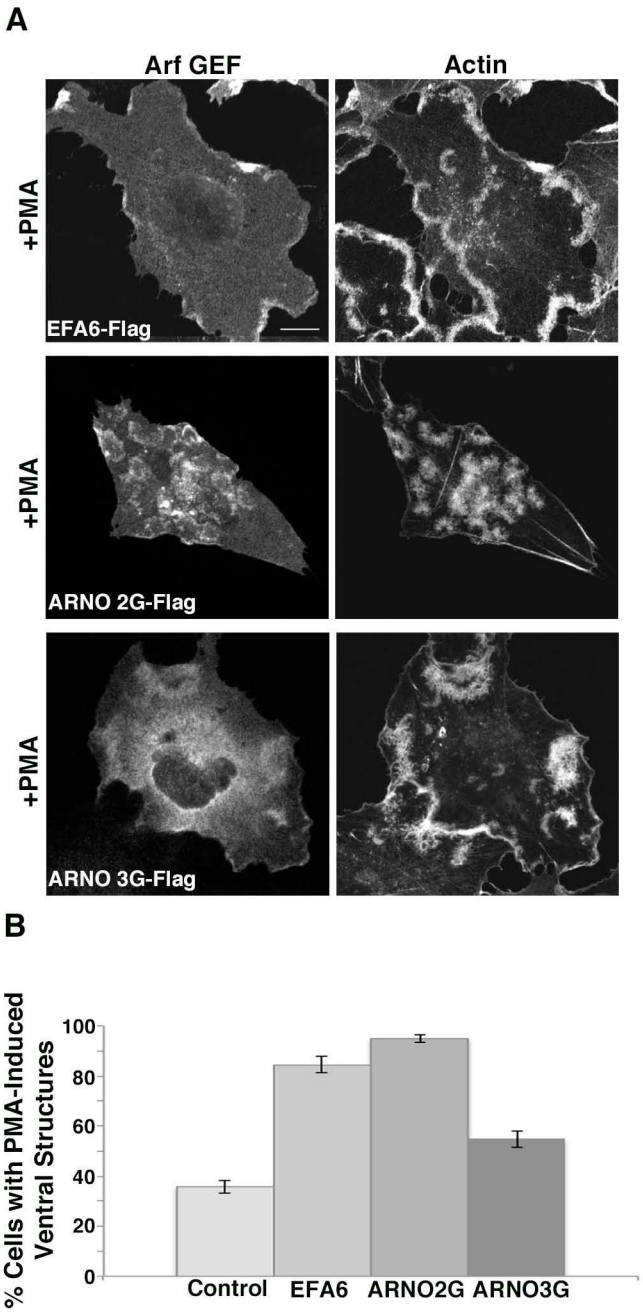

Figure 3. Arf GEFs enhance ventral actin structure formation in Beas-2b cells

(A) Beas 2B cells were transfected with plasmids encoding Flag-EFA6 (Arf6 GEF), or the Arf1 GEFS Flag-ARNO 2G (PIP_3 binding) or Flag-ARNO 3G (PIP_2 binding). Cells were treated with PMA, fixed and immunostained with antibody against Flag and rhodamine phalloidin. Bar, 10 μm. (B) Percentage of cells exhibiting one or more ventral actin structures was quantified. With the exception of Flag-EFA6, in total, 200 cells were counted from three independent experiments. For Flag-EFA6, in total, 123 cells were counted from three independent experiments. Error bars represent standard error for proportional data,

P<0.0001 as determined by Fisher's Exact test (two-sided) indicating that GEF expression resulted in increase in cells with ventral actin structures.

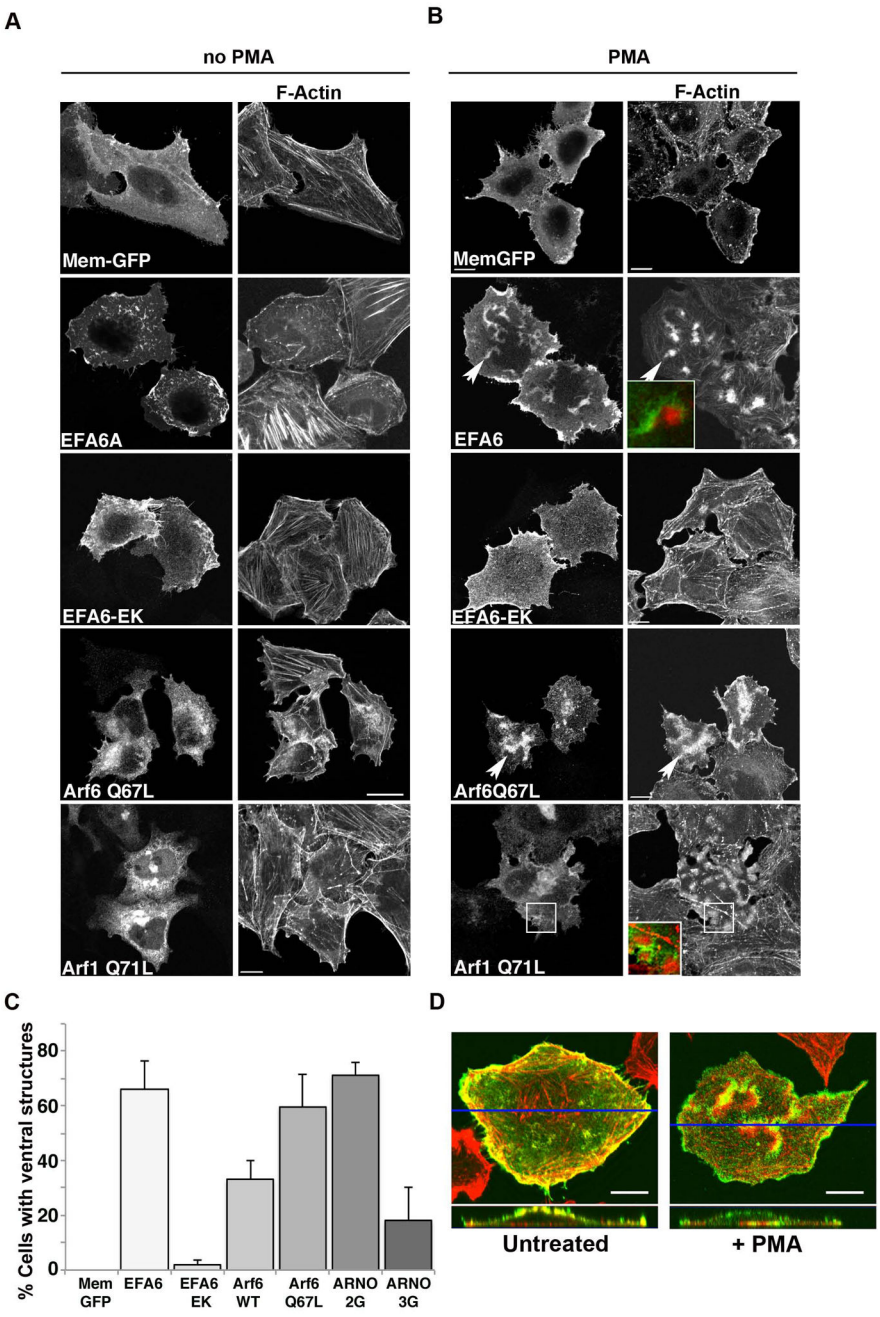

Figure 4. Active Arf6 or Arf1 promotes ventral actin structure formation in HeLa cells upon PMA treatment

HeLa cells were transfected with plasmids encoding Mem-GFP, FLAG-EFA6, FLAG-EFA6-EK, untagged Arf6 Q67L or Arf1Q71L-GFP. 18 hours following transfection, cells were untreated (A) or treated for 30 min with 200 nM PMA (B) prior to fixation and immunofluorescence staining as described in Materials and Methods. F-actin was labeled with rhodamine phalloidin, and antibodies to FLAG, Arf6 and Arf1 were detected with an Alexa 488-conjugated secondary antibody. In B arrow points to ventral ruffles, which are enlarged in inset. Bars,10 μm. (C) Fraction of cells expressing Mem-GFP, FLAG-EFA6,

FLAG-EFA6-EK, Arf6 Q67L, Arf1Q71L, FLAG-ARNO 2G or FLAG-ARNO 3G with 1 or more PMA-induced ventral actin structure visible by phalloidin staining was quantified and is expressed as the average percentage of transfected cells from three independent experiments with 100 cells scored in each experiment. Error bars represent one standard deviation from the mean. (D) Z-sections of HeLa cells, transfected with Flag-EFA6 that were untreated or treated with PMA for 15 min, fixed and stained with an antibody against Flag (green) and Rhodamine phalloidin (red). A cross-section of the cell shows that Flag-EFA6, which associates with the plasma membrane, shows increased concentration on the ventral (bottom) surface upon stimulation with PMA, where the ventral actin structure creates a membrane fold, or ruffle. A blue line denotes the location of the cross section.

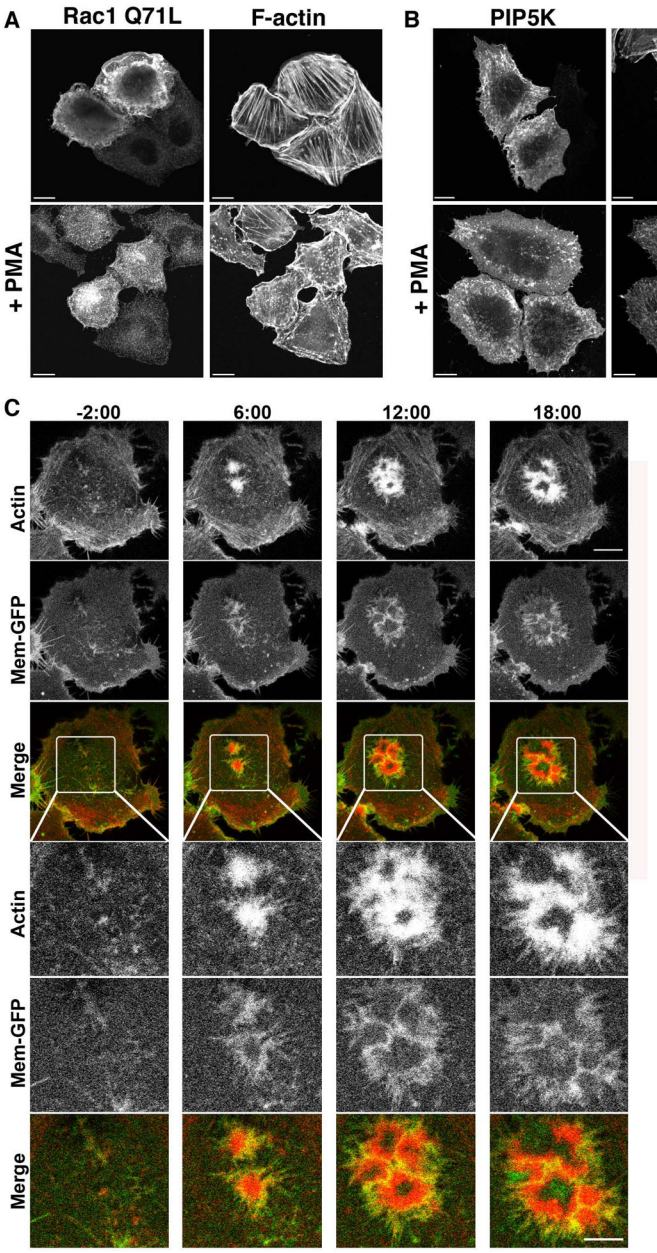

Figure 5. Rac1 and PIP5-kinase are not sufficient for ventral actin structures and actin and membrane dynamics in HeLa cells treated with PMA

HeLa cells expressing Rac1Q71L (A) or PIP5-kinase (PIP5K) (myc tagged) (B) were treated with 200 nm PMA for 30 min prior to fixation and immunofluorescence staining as described. Bars 10 μM. (C). HeLa cells coexpressing FLAG-EFA6 (in background), Mem-GFP (to label the membrane) and Life-Act-RFP (to label F-actin) were imaged live before and after addition of 100 nM PMA. PMA was added after 2 min, designated time 0, and frames were captured every 30 seconds thereafter. Selected stills from the movie at −2, 6,12 and 18 min are shown (see Movie 4 in Supplementary materials). Nascent actin structures visible at −2 min expand into larger actin structures after addition of PMA and by 6 min and

can be seen pushing a membrane fold outward. Bar, 10μM. Boxed regions are shown at higher magnification below each time point. Bar, 5 μM.

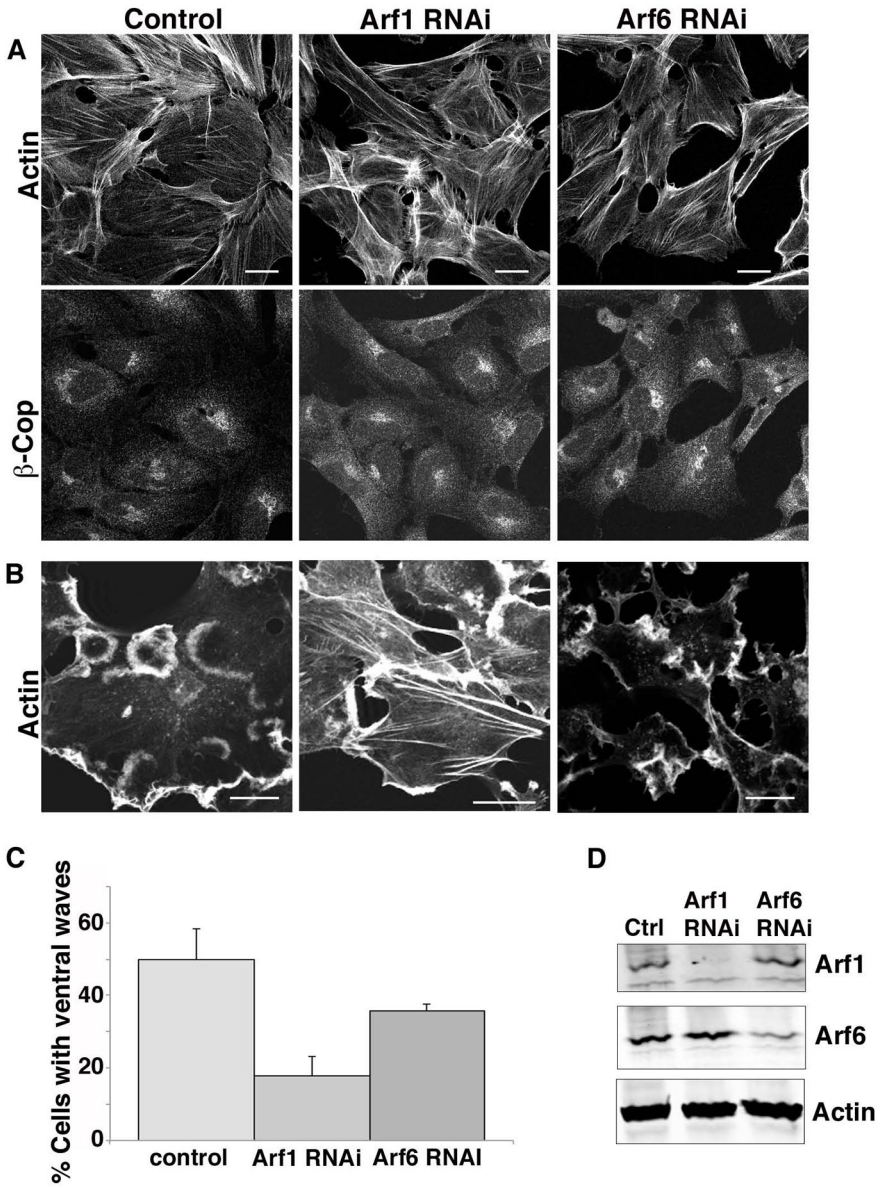

Figure 6. Arf1 and Arf6 are required for ventral wave formation in Beas-2b cells

(A) Beas-2b cells were transfected with siRNA to knockdown Arf1 or Arf6, or mock treated (control), as described in the Materials and Methods. 72 h after transfection, cells were fixed and stained by immunofluorescence as described in the Materials and Methods with an antibody against β-COP, and co-stained with rhodamine phalloidin. (B) Control and Arf1-or Arf6-depleted cells were treated with 200 nM PMA for 30 min prior to fixation and staining with rhodamine phalloidin. Bars,10 μm. (C) The fraction of 200 cells with 1 or more visible ventral waves was quantified and is expressed as the average percentage from three independent experiments. Error bars represent one standard deviation of the mean. One-way ANOVA revealed that both siRNA-depletions differed from control ($p<0.01$). (D) 5 X 10^5 cells were collected, lysed, and run on a SDS page gel, and immunoblotted with antibodies against Arf1, Arf6 and actin. Arf1 was depleted by 90% and Arf6 by 75%.

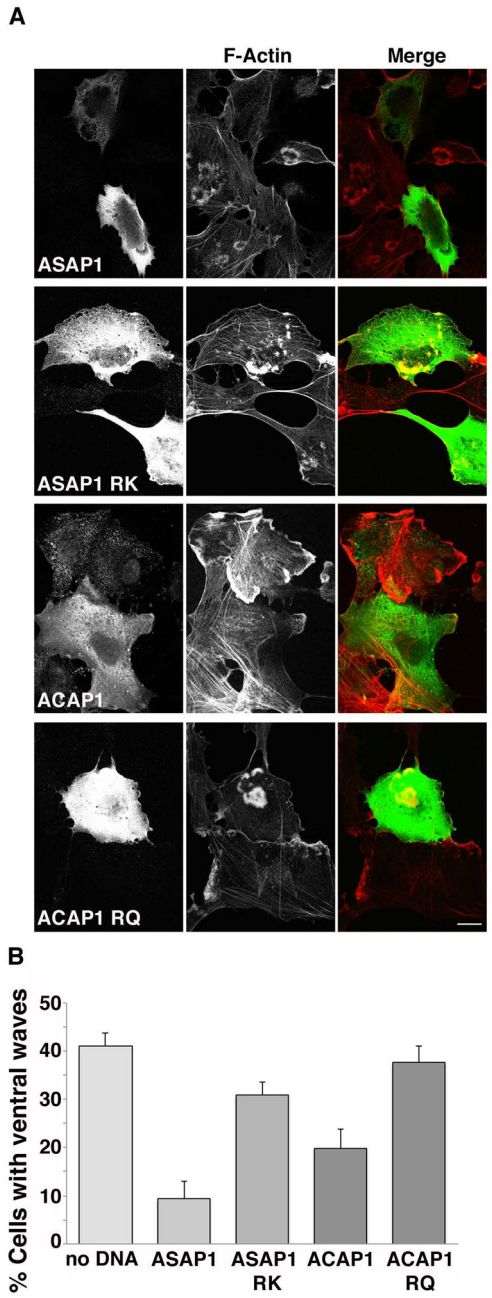

Figure 7. Expression of Arf GAPs inhibits ventral actin wave formation in Beas-2b cells

(A) Flag-ASAP1, Flag-ASAP1 RK, Flag-ACAP1 or Flag-ACAP1 RQ was transfected into Beas-2b cells. Cells were treated with PMA and stained with anti-Flag antibody (left column) and rhodamine phalloidin to detect F-actin (middle column). ASAP1 and ACAP1 transfected cells largely did not exhibit ventral actin waves, while cells transfected with enzymatically inactive control constructs ASAP1 RK and ACAP1RQ retained ventral actin waves. Bar, 10μm. (B) Quantification of percentage of control or transfected cells exhibiting ventral actin waves after PMA treatment. A minimum of 100 cells in total was counted from at least 3 independent experiments. Bars represent standard error for proportional data.

Percentage of cells transfected with ASAP1 or ACAP1 was significantly reduced compared to control cells ($P<0.0001$) as assessed by calculating P-values using Fisher's Exact test (two-tailed.) Percentage of cells expressing ASAP1 RK or ACAP1RQ exhibiting ventral waves was not statistically different than control cells.